

AGET ATRP of Poly[poly(ethylene glycol) methyl ether methacrylate] Catalyzed by Hydrophobic Iron(III)–Porphyrins

Ilaria Proietti Silvestri, Francesco Cellesi*

Received: July 28, 2015; Published online: September 21, 2015

1. Introduction

Since its discovery, atom transfer radical polymerization (ATRP) has become one of the most important methods for producing tailored vinyl polymers for industrial and biomedical use, with unprecedented control over composition, architecture, and functionality.^[1–3] Among different hydrophilic monomers, poly(ethylene glycol) methyl ether methacrylate (PEGMA) has been successfully employed in copper-mediated ATRP as biocompatible building block for the synthesis of advanced biocompatible materials.^[4–6] The precise design of functional PPEGMA with predetermined

molecular weight and well-defined architecture (homo, block, graft, and star polymers) has allowed its use in drug delivery, hydrogels, and surface modification of biomaterials.^[7–9] As in many other copper-catalyzed ATRP products, the synthesized PPEGMA may still contain traces of the residual copper after purification, and this may cause short-term and long-term toxicity to mammalian cells, animals and humans, thus limiting the applications in biology and medicine.^[7,10,11]

Intensive research has been carried out to reduce the amounts of transition metal used during the polymerization and to remove the residual catalyst from final products.^[1,7,11] On the other hand, biologically friendly iron may also be used to replace heavy metals in ATRP, although iron complexes are considered to be less efficient than copper catalysts in achieving controlled-living character.^[12]

In fact, iron-based catalysts can participate in multiple polymerization processes including ATRP, organometallic radical polymerization (OMRP), and catalytic chain transfer (CCT).^[12,13] The kinetics of these reactions seems

Dr. I. P. Silvestri, Prof. F. Cellesi
Fondazione CEN - European Centre for Nanomedicine
Piazza Leonardo da Vinci 32, 20133 Milan, Italy
E-mail: francesco.cellesi@polimi.it
Dr. I. P. Silvestri, Prof. F. Cellesi
Dipartimento di Chimica
Materiali ed Ingegneria Chimica “G. Natta,” Politecnico di
Milano, Via Mancinelli 7, 20131 Milan, Italy

to be strongly correlated with the metal spin state of the iron complex; in particular a high spin iron (III) state is desired to inhibit or at least minimize OMRP and CCT.^[12–16] Therefore, the catalytic properties of iron complexes depend on the combination of iron and coordinating ligands.^[12,17]

Several iron ligands have been used in ATRP, including phosphines and carbonyl complexes, onium salts, as well as amines.^[12,13] These iron complexes have been efficiently used for ATRP of hydrophobic monomers (i.e., styrene, methyl methacrylate), however they are often unable to effectively catalyze ATRP of hydrophilic monomers.^[12] Activator generated by electron transfer for ATRP (AGET ATRP), first introduced for copper-based catalysts,^[1] has also been reported for iron catalysts.^[12,18] In iron AGET ATRP the activator, i.e., the iron(II) complex, is generated by reducing the iron(III) complex with a reducing agent, such as the FDA-approved tin(II) 2-ethylhexanoate ($\text{Sn}(\text{Oct})_2$) or the nontoxic ascorbic acid.^[12] Iron AGET ATRP has the clear advantages of easy preparation, storage, and handling of the iron catalysts, and tolerance to limited amount of air (oxygen) during the reaction.^[19]

In this work, we investigated the feasibility of using commercially available, hydrophobic iron(III)–porphyrins as a versatile and “green” catalytic system for AGET ATRP of PEGMA.

Porphyrins are macroheterocyclic organic compounds, which form very stable complexes with transition metals,^[20,21] demonstrating catalytic activity in a variety of different reactions and in several fundamental biological processes.^[22,23] Iron(III)–porphyrins present a high spin state^[24,25] (for instance 5,10,15,20-tetraphenylporphyrin (TPP) and 2,3,7,8,12,13,17,18-octaethylporphyrin (OEP) show a spin state $S = 5/2$ for $\text{Fe-III}(\text{TPP})\text{Cl}$ and $\text{Fe-III}(\text{OEP})\text{Cl}$ complexes^[24]). The use of iron porphyrins as ATRP catalysts for bulk polymerization of methyl methacrylate and styrene has been reported in literature,^[26] as well as the use of bioinspired iron porphyrins (such as hemin and mesohemin-PEG) for ATRP of PEGMA in aqueous media.^[27] With mesohemin-PEG, PEGMA polymerizations showed good conversions with relatively low polydispersity index, although the synthesis of the catalysts required multiple reactions and purification steps. ATRP in aqueous media provides several advantages, since water is an environmentally benign solvent, which allows direct polymerization of hydrophilic monomers, even in the presence of proteins and other biomolecules. However, in many other cases, ATRP in organic solvent is preferred, particularly when hydrophilic and hydrophobic monomers need to be copolymerized and when polymers can be easily isolated by precipitation and solvent evaporation, thus avoiding tedious and expensive steps of dialysis, gel filtration chromatography, and freeze drying.

Here, combining advantages of using iron catalysts, AGET ATRP, and porphyrins as Fe(III) ligands, we report a novel facile strategy for the controlled synthesis of copper-free PEGMA-based macromolecules in organic solvent. Polymerizations mediated by commercially available, hydrophobic Iron(III)–porphyrin complexes were optimized in order to obtain conversions, average molecular weights, and polydispersity indexes comparable to standard copper-based ATRP. A “green” ATRP catalytic system, which involve ascorbic acid as a fully biocompatible Fe(III) reducing agent, despite its low solubility in organic phase, was also investigated as an alternative to AGET catalysts based on tin(II) 2-ethyl hexanoate.

2. Experimental Section

2.1. Materials

Poly(ethylene glycol) methyl ether methacrylate (PEGMA, average $M_n = 500$), stannous octoate ($\approx 95\%$), tetrabutylammonium bromide ($\geq 98\%$), 5,10,15,20-tetraphenyl-21*H*,23*H*-porphine iron(III) chloride ($\geq 94\%$), 5,10,15,20-tetrakis(4-methoxyphenyl)-21*H*,23*H*-porphine (95%), ethyl 2-bromo-2-methylpropionate (98%), L-ascorbic acid (reagent grade, powder), anisole (Reagent Plus, 99%), toluene (ACS Reagent, 99.7%), and tetrahydrofuran (THF) (HPLC grade, inhibitor free, 99.9%) were purchased from Sigma–Aldrich and used as received, unless otherwise stated.

PEGMA was passed through a column of neutral alumina to remove any inhibitors before use. Solvents were degassed by three freeze–pump–thaw cycles prior to use. Deionized water (18.2 M Ω) was obtained from a Millipore Milli-Q purification unit.

2.2. Synthesis of Fe^{III}-TMP

5,10,15,20-Tetrakis(4-methoxyphenyl)-21*H*,23*H*-porphine iron(III) chloride (Fe^{III}-TMP) was synthesized from 5,10,15,20-tetrakis(4-methoxyphenyl)-21*H*,23*H*-porphine (TMP) as previously reported in literature.^[28] Briefly, $\text{FeCl}_2 \cdot 4\text{H}_2\text{O}$ (162 mg, 0.816 mmol) was refluxed in acetonitrile (25 mL) under N_2 for 1 h. After cooling the temperature to 70 °C, a suspension of TMP (150 mg, 0.204 mmol) in degassed dichloromethane (12 mL) was added through a dropping funnel under N_2 . The reaction mixture was stirred at 70 °C for 30 min, then was cooled to room temperature and exposed to the air for further 30 min. The reaction mixture was diluted with dichloromethane and the organic layer was washed twice with HCl 0.2 N and water. The organic layer was dried over Na_2SO_4 and the solvent evaporated under vacuum. The brownish residue was dissolved in dichloromethane and precipitated in an excess of hexane yielding Fe^{III}-TMP (104 mg, 62%) as a dark purple solid.

2.3. General Polymerization Procedure for Screening Reactions Using Stannous Octoate

A series of AGET ATRP reactions using PEGMA monomer was carried out under different experimental conditions. A typical polymerization procedure (identified by the

molar ratios $[\text{PEGMA}]_0:[\text{EBiB}]_0:[\text{TBABr}]:[\text{Fe}^{\text{III}}\text{-TPP}]:[\text{Sn}(\text{Oct})_2] = 100:1:50:1:1$ was as follows: PEGMA (1 g, 2.0 mmol), 5,10,15,20-tetraphenyl-21*H*,23*H*-porphine iron(III) chloride ($\text{Fe}^{\text{III}}\text{-TPP}$ 14 mg, 0.02 mmol) and tetrabutylammonium bromide (TBABr, 322 mg, 1 mmol) were added to a Schlenk flask wrapped in aluminum foil, which was evacuated and backfilled with nitrogen three times. Degassed anisole (5 mL) was added and the flask was sealed with a rubber septum and placed in an oil bath at 60 °C under stirring. Stannous octoate (8 mg, 0.02 mmol) and ethyl 2-bromo-2-methylpropionate (EBiB) were added under nitrogen atmosphere and the reaction was allowed to stir for 7.5 h. Aliquots (100 μL sample) were withdrawn from the reaction mixture at intervals during the course of the reaction, filtered through a pad of neutral alumina, and analyzed by ^1H NMR spectroscopy using CDCl_3 as a deuterated solvent to measure conversion and to examine the evolution of molecular weight. The concentrations of the reactants (monomer vinyl signals at $\delta = 5.5$ and 6.0 ppm $\text{CH}_2=\text{C}(\text{CH}_3)-$) compared to the product (broad singlet at $\delta = 4.07$, $-\text{CH}_2\text{C}=\text{O}$) were calculated with respect to reaction time by ^1H NMR analysis. At the end of the polymerization, the reaction mixture was quenched by cooling the flask at -20 °C, and passed through a pad of neutral alumina to remove the catalyst. The filtrate was concentrated and the residue was precipitated from hexane. The polymer obtained was dried in vacuum. The catalyst removal was confirmed by UV-vis spectroscopy and the pure polymer was characterized by ^1H NMR (see Figures S1 and S2, Supporting Information).

2.4. Chain Extension of Poly(PEGMA)

Poly(PEGMA)-Br macroinitiator was obtained by $\text{Sn}(\text{Oct})_2/\text{Fe}^{\text{III}}\text{-TPP}$ -mediated polymerization using $[\text{PEGMA}]_0:[\text{TBABr}]:[\text{Sn}(\text{Oct})_2]:[\text{Fe}^{\text{III}}\text{-TPP}]:[\text{EBiB}] = 100:50:10:1:1$, $[\text{PEGMA}]_0 = 0.4$ M in anisole at 60 °C. The reaction was stopped after 60 min (thus obtaining a monomer conversion of 40%). The polymer solution was passed through neutral alumina and precipitated in hexane. After filtration and drying at rotary evaporator, the purified macroinitiator ($M_n = 13379$, PDI = 1.08, according to GPC analysis) was added to a Schlenk flask together with PEGMA monomer (1 g, 2.0 mmol), $\text{Fe}^{\text{III}}\text{-TPP}$ (14 mg, 0.02 mmol) and TBABr (322 mg, 1 mmol). The flask was wrapped in aluminum foil and evacuated and backfilled with nitrogen three times. Degassed anisole (5 mL) was added and the flask was sealed with a rubber septum and placed in an oil bath at 60 °C under stirring. Stannous octoate (80 mg, 0.2 mmol) was added under nitrogen atmosphere and the reaction was allowed to stir for 7.5 h. The polymerization was quenched by cooling the flask at -20 °C, then the reaction mixture was passed through a pad of neutral alumina to remove the catalyst. The filtrate was concentrated and the residue was precipitated in hexane. The polymer obtained was dried in vacuum and analyzed by GPC ($M_n = 20\,965$ and PDI = 1.04).

2.5. General Polymerization Procedure for Screening Reactions Using Ascorbic Acid

A typical polymerization procedure (identified by the molar ratios $[\text{PEGMA}]_0:[\text{EBiB}]_0:[\text{TBABr}]:[\text{Fe}^{\text{III}}\text{-TPP}]:[\text{AscAc}] = 100:1:50:1:1$) was as follows: PEGMA (1 g, 2.0 mmol), $\text{Fe}^{\text{III}}\text{-TPP}$ (14 mg, 0.02 mmol),

l-ascorbic acid (35 mg, 0.02 mmol), and TBABr (322 mg, 1 mmol) were added to a Schlenk flask wrapped in aluminum foil, which was evacuated and backfilled with nitrogen three times. Degassed anisole (5 mL or 0.5 mL, depending on reaction conditions) and a fixed amount of degassed water (when required, depending on reaction conditions) were added and the flask was sealed with a rubber septum and placed in an oil bath at 60 °C under stirring. EBiB was added under nitrogen atmosphere and the reaction was allowed to stir for 7.5 h. Aliquots were taken at intervals to measure conversion and to examine the evolution of molecular weight, as described above. The polymerization was quenched by cooling the flask at -20 °C, and then the reaction mixture was passed through a pad of neutral alumina to remove the catalyst. The filtrate was concentrated and the residue was precipitated in hexane. The polymer obtained was dried in vacuum.

2.6. Characterization

The number-average molecular weight ($M_{n,\text{GPC}}$) values and molecular weight distributions (M_w/M_n) values of the polymers were evaluated using a Jasco LC-2000Plus gel permeation chromatograph (GPC) equipped with a refractive index detector (RI-2031Plus, Jasco) using 3 Agilent PLgel columns, 5×10^{-6} M particle size, 300×7.5 mm (M_w range: 5×10^2 to 17×10^5 g mol $^{-1}$). THF was chosen as eluent at a flow rate of 0.5 mL min $^{-1}$ at 35 °C. The GPC samples were injected using a Jasco AS-2055Plus autosampler. The instrument was calibrated using polystyrene standards.

^1H NMR spectra were recorded on a Bruker Avance 400 MHz and 500 MHz NMR instruments, using CDCl_3 as a solvent. The solvent residual peak was used as internal standard.

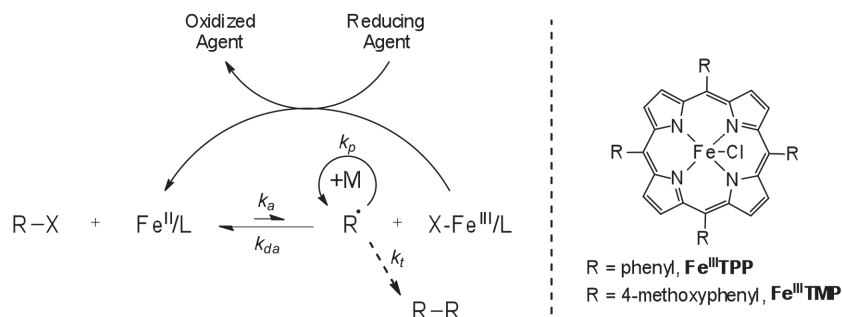
UV-vis spectra were recorded on a Jasco V-630 spectrophotometer from 290 to 900 nm.

3. Results and Discussion

3.1. PEGMA Polymerization Using $\text{Sn}(\text{Oct})_2$ as a Reducing Agent

5,10,15,20-Tetrakis(4-methoxyphenyl)-21*H*,23*H*-porphine iron(III) chloride ($\text{Fe}^{\text{III}}\text{-TMP}$) and 5,10,15,20-tetraphenyl-21*H*,23*H*-porphine iron(III) chloride ($\text{Fe}^{\text{III}}\text{-TPP}$) (see Scheme 1) were firstly investigated as catalysts in AGET ATRP of PEGMA ($M_n = 500$ g mol $^{-1}$) in anisole.

PEGMA was polymerized at 60 °C from commercial ethyl 2-bromoisobutyrate (EBiB) initiator in presence of stannous octoate as a reducing agent (using equimolar amount of $\text{Sn}(\text{Oct})_2$ and porphyrin). An excess of TBABr was also added to shift the equilibrium of iron-chloride to iron-bromide species, enhancing the efficiency of deactivation and initiation, and overcoming possible limitations due to the low halidophilicity of $\text{Fe}(\text{III})$ porphyrins.^[27] $\text{Fe}^{\text{III}}\text{-TPP}$ gave excellent polydispersity index (PDI = 1.12) with a conversion of 31% after 7.5 h, while $\text{Fe}^{\text{III}}\text{-TMP}$ gave a slightly lower conversion (25% after



Scheme 1. Proposed mechanism for Fe-mediated AGET-ATRP and porphyrin-based catalysts structure.

7.5 h) still maintaining a good PDI value (1.13). In order to compare the activity of porphyrins to another macroheterocycle with lower spin state,^[29] iron(III) phthalocyanin was tested as catalyst under the same reaction condition, although it was unable to initiate the polymerization (Table 1, entries 1–3).

Toluene and THF were also used as organic solvents for Fe-ATRP. Compared to anisole, the less polar toluene did not lead to a significant variation of conversion (30%–34% in 7.5 h) even when the temperature was increased from 60 °C to 80 °C. On the other hand, polymerization in THF did not occur (Table 2), possibly because of a negative effect of the THF binding to the iron–porphyrin complex.^[30,31]

Due to the encouraging results obtained with Fe(III)-TPP and Sn(Oct)₂, we tested the effect of the amount of the reducing agent on the polymerization. As expected, the initiation did not occur in absence of Sn(Oct)₂, but conversion was markedly raised by increasing Sn(Oct)₂ concentration, reaching 85% in 7.5 h when the molar amount of stannous octoate was 10 times the catalyst (Table 1, entries 4–7). We registered a little increment of the PDI, but the polymerization was still

under good control (PDI < 1.2). Despite the large excess of reducing agent used, these experimental conditions allowed the synthesis of PPEGMA at higher conversion and lower PDI than those reported in other works on Fe-ATRP of PEGMA in water,^[7,27] in anisole^[27] and in bulk.^[7,32]

In terms of average-number molecular weights, it has to be noted that with Fe(III)-TPP-based polymerizations, the M_n calculated by GPC differ substantially from the theoretical values; in particular low M_n values were found at high monomer conversion, which may be ascribed to the presence of catalytic chain-transfer mechanisms typical of iron catalysts.^[14] Polymerization kinetics were therefore investigated to assess the controlled/living behavior of these ATRP. The kinetic plot of $\ln([M]_0/[M])$

Table 1. Polymerization of PEGMA mediated by Fe^{III} catalyst and Sn(Oct)₂ in anisole.

Entry	[Sn(Oct) ₂]:[Cat] ^{a)}	Conversion [%] ^{b)}	$M_{n,th}$ ^{c)}	$M_{n,GPC}$	M_w	PDI
1 ^{d)}	1:1	31	15 500	9315	10 417	1.12
2 ^{e)}	1:1	25	12 500	9360	10 551	1.13
3 ^{f)}	1:1	0	—	—	—	—
4 ^{d)}	0:1	0	—	—	—	—
5 ^{d)}	1:1	30	15 000	11 166	12 417	1.11
6 ^{d)}	4:1	67	33 500	10 532	12 441	1.18
7 ^{d)}	10:1	85	42 500	14 784	17 609	1.19

^{a)}General conditions [PEGMA]₀: [TBABr]: [Cat]: [EBiB] = 100:50:1:1. [PEGMA]₀ = 0.4 M in anisole. *T* = 60 °C, 7.5 h; ^{b)}Conversion; and ^{c)}theoretical number-average molecular weight $M_{n,th}$ were determined by ¹H NMR; ^{d)}Cat = Fe^{III}-TPP; ^{e)}Cat = Fe^{III}-TMP; ^{f)}Cat = iron(III) phthalocyanin.

Table 2. Polymerization of PEGMA mediated by Fe^{III}-TPP and TBABr in different solvents.

Entry	Solvent ^{a)}	<i>T</i> [°C]	Conv. [%] ^{b)}	$M_{n,th}$ ^{c)}	$M_{n,GPC}$	M_w	PDI
1	THF	60	0	—	—	—	—
2	Toluene	60	34	17 000	15 584	17 939	1.15
3	Toluene	80	35	17 500	11 010	12 469	1.13
4	Anisole	60	30	15 000	11 166	12 417	1.11

^{a)}General conditions [PEGMA]₀ = 0.4 M [PEGMA]₀: [TBABr]: [Sn(Oct)₂]: [Fe^{III}-TPP]: [EBiB] = 100:50:1:1:1. Reaction time 7.5 h; ^{b)}Conversion; and ^{c)}theoretical number average molecular weight $M_{n,th}$ were determined by ¹H NMR.

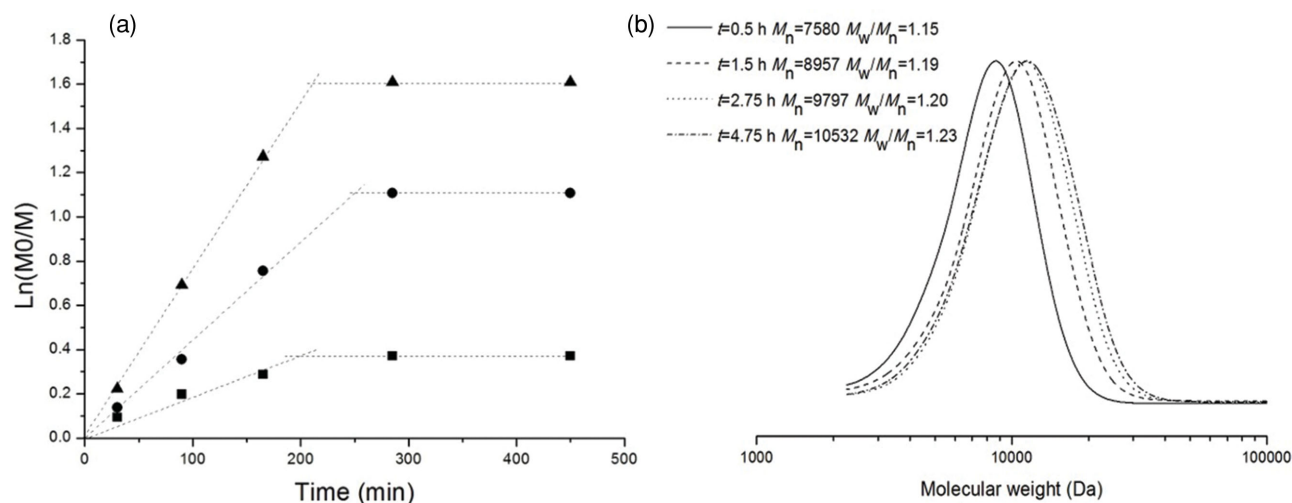


Figure 1. A) Kinetic plot of $\ln([M]_0/[M])$ versus time for PEGMA polymerization using Fe^{III} -TPP and 1 (■), 4 (●) and 10 equiv (▲) of $\text{Sn}(\text{Oct})_2$. B) GPC chromatograms of PPEGMA in anisole (20% v/v). $[\text{PEGMA}]_0:[\text{Sn}(\text{Oct})_2]:[\text{EBiB}]:[\text{TBABr}]:[\text{Fe}^{\text{III}}\text{-TPP}] = 100:4:1:50:1$; $T = 60^\circ\text{C}$ (t = reaction time).

as a function of time (Figure 1) showed linearity within the first 3.5–4 h of reaction, indicating first-order kinetics with constant concentration of active centers until the maximum conversion was reached, after which the curves plateaued, thus indicating possible termination. The kinetic constant of the polymerization (k_{obs}) increased with the increase of reducing agent concentration ($k_{\text{obs}} = 7.8 \times 10^{-3} \text{ s}^{-1}$, $4.6 \times 10^{-3} \text{ s}^{-1}$, and $1.4 \times 10^{-3} \text{ s}^{-1}$ using 10, 4, and 1 equivalent of $\text{Sn}(\text{Oct})_2$ respectively). This is in agreement with the ATRP mechanism where the propagation rate is proportional to the ratio of the concentration of reduced and oxidized species $[\text{Fe}(\text{II})\text{L}]/[\text{Fe}(\text{III})\text{L-Br}]$, which is clearly affected by the $\text{Sn}(\text{Oct})_2$ concentration. The GPC traces of PPEGMA were monomodal and characterized by a rather narrow polydispersity ($\text{PDI} < 1.23$, Figure 2).

The need to use a large excess of tetrabutylammonium bromide to enhance polymerization efficiency was confirmed experimentally. As expected, by reducing the molar ratio $[\text{TBABr}]:[\text{Fe}^{\text{III}}\text{-TPP}]$ from 50:1 to 0 we noticed a decrease of conversion from 85% to 54% (Table 3). Since tetrabutylammonium bromide was also used as ligand in iron-mediated ATRP,^[33] polymerizations with TBABr in absence of porphyrin (entry 5, Table 3), as well as without TBABr and in absence of any other ligand (entry 6, Table 3) were also carried out for comparison. The poor ability of TBABr to catalyze the reaction without TPP was confirmed by the very low conversion obtained (6%), whereas the only presence of FeCl_2 as a source of iron without any complexing agent was not sufficient to initiate the polymerization, as expected.

A chain extension experiment was performed to confirm the chain-end functionality of PPEGMA and to verify the living character of these polymerizations. PPEGMA

($M_n = 13\,379$, $\text{PDI} = 1.08$) was isolated from an ATRP optimized for the Fe^{III} -TPP/ $\text{Sn}(\text{Oct})_2$ system and used as macroinitiator for further PEGMA polymerization. The reinitiation appeared complete, yielding PPEGMA at higher molecular weight but still at low polydispersity ($M_n = 20\,965$ and $\text{PDI} = 1.04$), with no evidence of dead chains in the GPC chromatogram (Figure 3).

3.2. PEGMA Polymerization Using Ascorbic Acid as a Reducing Agent

Furthermore, ascorbic acid was tested as more biocompatible alternative to $\text{Sn}(\text{Oct})_2$. The effect of ascorbic acid on PEGMA polymerization was screened using Fe^{III} -TPP

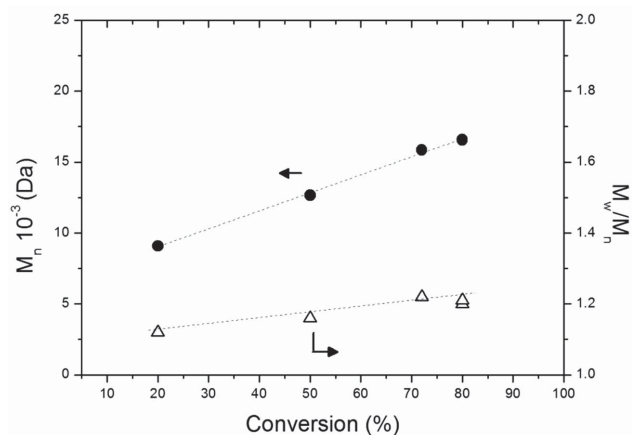


Figure 2. M_n and PDI vs conversion for PEGMA polymerization DP 100 in anisole (20% v/v), using Fe^{III} -TPP and 10 equivalents of $\text{Sn}(\text{Oct})_2$.

Table 3. Polymerization of PEGMA mediated by Fe^{III}-TPP—Effect of TBABr amount.

Entry	[TBABr]:[Fe ^{III}] ^{a)}	Conv. [%] ^{b)}	$M_{n,th}$ ^{c)}	$M_{n,GPC}$	M_w	PDI
1 ^{d)}	50:1	85	42 500	14 784	17 609	1.19
2 ^{d)}	25:1	71	35 500	15 473	17 039	1.10
3 ^{d)}	1:1	62	31 000	14 605	16 703	1.14
4 ^{d)}	0:1	54	27 000	13 194	14 777	1.12
5 ^{e)}	50:1	6	3000	10 825	12 744	1.18
6 ^{e)}	0:1	0	—	—	—	—

^{a)}General conditions [PEGMA]₀: [Sn(Oct)₂]: [Fe^{III}-TPP]: [EBiB] = 100:10:1:1; *T* = 60 °C, 7.5 h. [PEGMA] = 0.4 M in anisole; ^{b)}Conversion; and ^{c)}theoretical number average molecular weight $M_{n,th}$ were determined by ¹H NMR; ^{d)}TPP was used as ligand; ^{e)}FeCl₂ was used as source of iron, in absence of TPP.

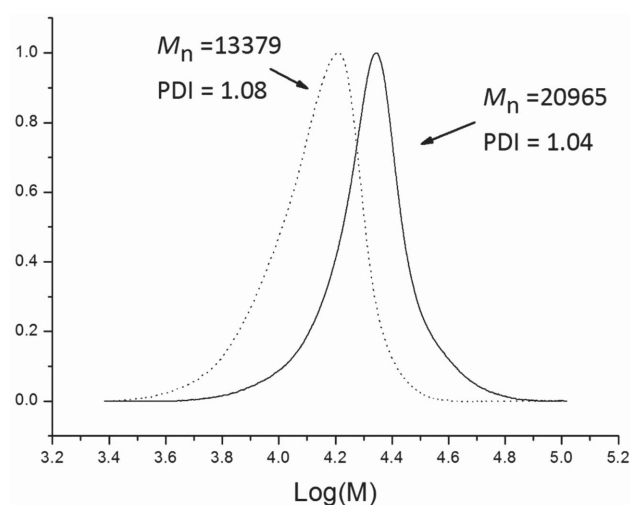


Figure 3. GPC chromatograms PEGMA before (dotted line) and after (solid line) chain extension.

as a catalyst, due to its high activity with Sn(Oct)₂ and its convenient commercial availability as metalloporphyrin (whereas the commercial TMP required an additional synthetic step for iron insertion). By using equimolar amounts of ascorbic acid and Fe^{III}-TPP in anisole only 15% conversion was obtained (PDI = 1.12, Table 4). As with stannous octoate, conversion improved with the amount of ascorbic acid employed, but even an excess of 10 to 1 could not increase the conversion over 26%.

These low conversions were ascribed to the scarce solubility of ascorbic acid in the reaction media. Therefore, we firstly attempted to improve solubility by reducing the ratio between the hydrophobic anisole and the hydrophilic PEGMA, although only a limited increment of conversion was observed (see entry 1 and entry 7, Table 4). Second, we attempted to increase the solubility of ascorbic acid by adding small amounts of water to the reaction system. It should be noted that the presence

Table 4. Polymerization of PEGMA mediated by Fe^{III}-TPP (Cat) and ascorbic acid (Red).

Entry	Solvent	[Red]:[Cat] ^{a)}	Conv. [%] ^{b)}	$M_{n,th}$ ^{c)}	$M_{n,GPC}$	M_w	PDI
1	Anisole	1:1	15	7500	7001	7832	1.12
2	Anisole	4:1	20	10 000	8577	9210	1.07
3	Anisole	10:1	26	13 000	8700	9274	1.07
4	Anisole/H ₂ O ^{d)}	1:1	19	9500	11 298	12 708	1.12
5	Anisole/H ₂ O ^{e)}	1:1	35	17 500	12 342	14 060	1.14
6	Anisole/H ₂ O ^{f)}	1:1	42	21 000	15 186	18 435	1.21
7	Anisole ^{g)}	1:1	20	10 000	8311	9070	1.09
8	Anisole/H ₂ O ^{g,h)}	1:1	34	17 000	12 180	13 843	1.14
9	Anisole/H ₂ O ^{g,i)}	1:1	39	19 500	12 493	14 307	1.15
10	Anisole/H ₂ O ^{g,j)}	1:1	64	32 000	21 265	23 905	1.13

^{a)}General conditions [PEGMA]₀: [TBABr]: [Fe^{III}-TPP]: [EBiB] = 100:50:1:1. [PEGMA]₀ = 0.4 M in anisole. *T* = 60 °C, 7.5 h; ^{b)}Conversion; and ^{c)}theoretical number-average molecular weight $M_{n,th}$ were determined by ¹H NMR; ^{d)} Anisole:H₂O = 1000:1 (v/v); ^{e)}Anisole:H₂O = 500:1 (v/v); ^{f)}Anisole:H₂O = 100:1 (v/v); ^{g)}[PEGMA]₀ = 4 M in anisole; ^{h)}Anisole:H₂O = 100:1 (v/v); ⁱ⁾ Anisole:H₂O = 50:1 (v/v); ^{j)}Anisole:H₂O = 10:1 (v/v).

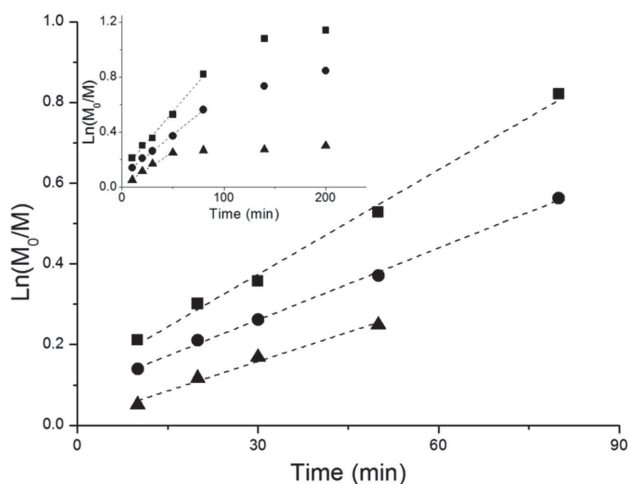


Figure 4. Kinetic plot of $\ln([M]_0/[M])$ versus time for PEGMA polymerization using Fe^{III} -TPP and ascorbic acid, at different degree of polymerization (inset; data collected up to 320 min); DP 50 (■), 100 (●) and 200 (▲). General conditions $[\text{PEGMA}]_0:[\text{TBABr}]:[\text{Fe}^{\text{III}}\text{-TPP}]:[\text{EBiB}] = 100:50:1:1$. $[\text{PEGMA}]_0 = 4 \text{ M}$ in anisole. Anisole: H_2O 10:1 (v/v).

of the amphiphilic TBABr, as well as PEGMA, favored water dispersibility, and even at a ratio anisole/water 10:1, v/v ($[\text{PEGMA}]_0 = 4 \text{ M}$ in anisole), no phase separation was noticed. By adding a variable amount of water (0.005–0.05 mL) to a fixed amount of anisole (5 mL) the conversion progressively improved up to 42%, together with a slight increase of PDI (from 1.12 to 1.21, entries 4–6 Table 4). Conversion was further increased when the same amounts of water were added to a much lower amount of anisole (0.5 mL, entries 8–10 Table 4), and the maximum conversion (64%) was obtained for anisole: $\text{H}_2\text{O} = 10:1$ v/v (entry 10, Table 4). Similarly to what observed in $\text{Sn}(\text{Oct})_2$ -based polymerizations, at high conversions the experimental M_n were lower than the theoretical

values, however this gap was significantly reduced by using ascorbic acid instead of $\text{Sn}(\text{Oct})_2$.

Kinetic studies were undertaken with the Fe^{III} -TPP/ascorbic acid system. $\ln[M]_0/[M]$ versus time showed a linear trend for three different targeted degrees of polymerization (DP = 50, 100, and 200), indicating a constant number of active species during the first 60–90 min of reaction (Figure 4). Full monomer conversion was never reached, and the kinetic curves approached to a plateau after 200 min (inset, Figure 4), suggesting the presence of termination reactions. A faster polymerization kinetics was also noticed within the first few minutes, taking into account that a linear regression of the experimental data did not return a zero intercept. The complexity of the polymerization kinetics, due to the interplay of different metal-catalyzed reaction mechanisms, was also confirmed by showing the evolution of the number-average molecular weight (DP = 100, Figure 5), highlighting a linear relationship between M_n and conversion but also an unexpected high M_n at the beginning of the polymerization. Molecular weight distributions remained narrow during the reaction, although a linear increase of the PDI with conversion was observed (Figure 5).

4. Conclusion

Iron-mediated AGET ATRP of PEGMA in organic solvent was successfully developed using commercially available porphyrins as $\text{Fe}(\text{III})$ ligand. When tin(II) 2-ethyl hexanoate was used as a reducing agent, linear brush-like macromolecules with narrow molecular weight distributions ($M_w/M_n \leq 1.2$) and high monomer conversion (up to 85%) were obtained. The key features of these polymerizations were investigated by monitoring kinetics as well as the

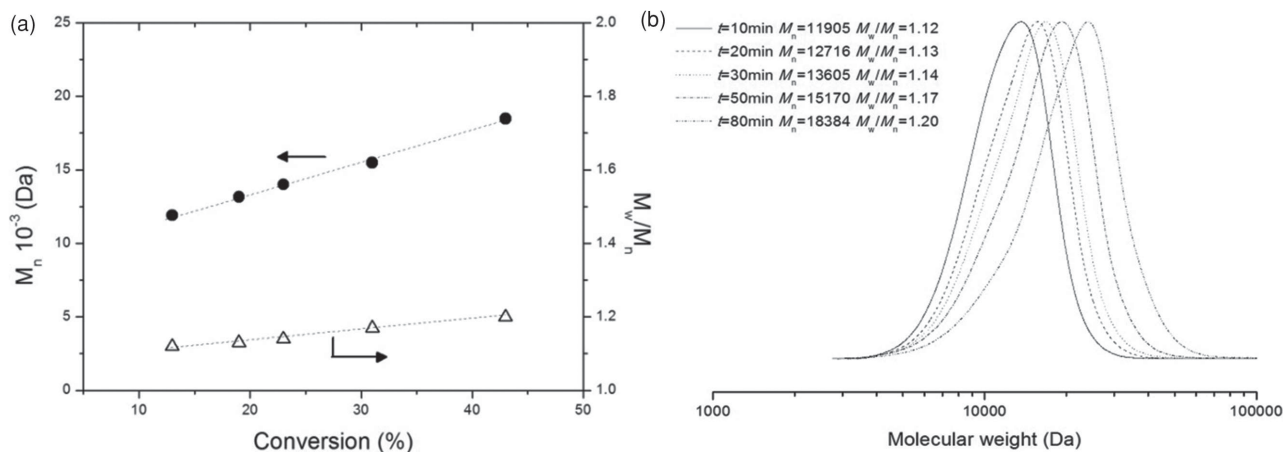


Figure 5. A) M_n and PDI vs. conversion for DP 100 for PEGMA polymerization using Fe^{III} -TPP and ascorbic acid. B) Details of the GPC chromatograms. General conditions $[\text{PEGMA}]_0:[\text{TBABr}]:[\text{Fe}^{\text{III}}\text{-TPP}]:[\text{EBiB}] = 100:50:1:1$. $[\text{PEGMA}]_0 = 4 \text{ M}$ in anisole. Anisole: H_2O 10:1 (v/v).

chain-extension capability of the synthesized PPEGMA. Ascorbic acid was also tested as more biocompatible alternative to Sn(Oct)₂ in reducing Fe(III). By adding small amount of water to increase the solubility of ascorbic acid in the organic reactant dispersion, good monomer conversion (64%) and relatively low polydispersity index (≤ 1.2) were also obtained. This environmentally friendly ATRP catalytic system may represent a valuable tool for the design and synthesis of copper-free PEG-based biomaterials, with high control over architecture, composition, and functionality.

Supporting Information

Supporting Information is available from the Wiley Online Library or from the author.

Acknowledgements: The financial support from Fondazione CEN - European Centre for Nanomedicine (Start-up package grant), co-funded by Regione Lombardia through the "Fondo per lo sviluppo e la coesione 2007–2013" is gratefully acknowledged. The authors thank Prof. Giuseppe Storti (ETH, Zurich) for assistance with GPC analysis and fruitful discussion.

- [1] K. Matyjaszewski, *Macromolecules* **2012**, *45*, 4015.
- [2] J.-S. Wang, K. Matyjaszewski, *J. Am. Chem. Soc.* **1995**, *117*, 5614.
- [3] L. Ragupathy, D. G. Millar, N. Tirelli, F. Cellesi, *Macromol. Biosci.* **2014**, *14*, 1528.
- [4] J. K. Oh, K. Min, K. Matyjaszewski, *Macromolecules* **2006**, *39*, 3161.
- [5] J.-F. Lutz, *J. Polym. Sci., Part A: Polym. Chem.* **2008**, *46*, 3459.
- [6] H. Hussain, K. Y. Mya, C. He, *Langmuir* **2008**, *24*, 13279.
- [7] W. He, L. Zhang, J. Miao, Z. Cheng, X. Zhu, *Macromol. Rapid Commun.* **2012**, *33*, 1067.
- [8] M.-C. Jones, M. Ranger, J.-C. Leroux, *Bioconjugate Chem.* **2003**, *14*, 774.
- [9] J. Miao, W. He, L. Zhang, Y. Wang, Z. Cheng, X. Zhu, *J. Polym. Sci., Part A: Polym. Chem.* **2012**, *50*, 2194.
- [10] B. R. Stern, M. Solioz, D. Krewski, P. Aggett, T.-C. Aw, S. Baker, K. Crump, M. Dourson, L. Haber, R. Hertzberg, C. Keen, B. Meek, L. Rudenko, R. Schoeny, W. Slob, T. Starr, *J. Toxicol. Environ. Health Part B: Crit. Rev.* **2007**, *10*, 157.
- [11] N. V. Tsarevsky, K. Matyjaszewski, *Chem. Rev.* **2007**, *107*, 2270.
- [12] Z. Xue, D. He, X. Xie, *Polym. Chem.* **2015**, *6*, 1660.
- [13] F. di Lena, K. Matyjaszewski, *Prog. Polym. Sci.* **2010**, *35*, 959.
- [14] R. Poli, *Angew. Chem. Int. Ed.* **2006**, *45*, 5058.
- [15] M. P. Shaver, L. E. N. Allan, H. S. Rzepa, V. C. Gibson, *Angew. Chem. Int. Ed.* **2006**, *45*, 1241.
- [16] M. P. Shaver, L. E. N. Allan, V. C. Gibson, *Organometallics* **2007**, *26*, 4725.
- [17] R. Poli, L. E. N. Allan, M. P. Shaver, *Prog. Polym. Sci.* **2014**, *39*, 1827.
- [18] L. Zhang, Z. Cheng, F. Tang, Q. Li, X. Zhu, *Macromol. Chem. Phys.* **2008**, *209*, 1705.
- [19] Z. Deng, J. Guo, L. Qiu, C. Yuan, Y. Zhou, F. Yan, *J. Polym. Sci., Part A: Polym. Chem.* **2013**, *51*, 664.
- [20] M. Biesaga, K. Pyrzyńska, M. Trojanowicz, *Talanta* **2000**, *51*, 209.
- [21] F. A. Walker, U. Simonis, in *Encyclopedia of Inorganic and Bioinorganic Chemistry*, John Wiley & Sons, Ltd., Hoboken, NJ, USA, **2011**.
- [22] X. Huang, K. Nakanishi, N. Berova, *Chirality* **2000**, *12*, 237.
- [23] H. X. Sheng, R. E. Chaparro, T. Sasaki, M. Izutsu, R. D. Pearlstein, A. Tovmasyan, D. S. Warner, *Antioxid. Redox Signaling* **2014**, *20*, 2437.
- [24] R. J. Cheng, P. Y. Chen, P. R. Gau, C. C. Chen, S. M. Peng, *J. Am. Chem. Soc.* **1997**, *119*, 2563.
- [25] D. Sahoo, M. G. Quesne, S. P. de Visser, S. P. Rath, *Angew. Chem. Int. Ed. Engl.* **2015**, *54*, 4796.
- [26] R. M. Islamova, S. V. Nazarova, O. I. Koifman, *Macroheterocycles* **2011**, *4*, 97.
- [27] A. Simakova, M. Mackenzie, S. E. Averick, S. Park, K. Matyjaszewski, *Angew. Chem. Int. Ed.* **2013**, *52*, 12148.
- [28] N. Asano, S. Uemura, T. Kinugawa, H. Akasaka, T. Mizutani, *J. Org. Chem.* **2007**, *72*, 5320.
- [29] B. J. Kennedy, K. S. Murray, P. R. Zwack, H. Homborg, W. Kalz, *Inorg. Chem.* **1986**, *25*, 2539.
- [30] C. Lecomte, R. H. Blessing, P. Coppens, A. Tabard, *J. Am. Chem. Soc.* **1986**, *108*, 6942.
- [31] D. Brault, M. Rougee, *Biochemistry* **1974**, *13*, 4591.
- [32] J. Pan, J. Miao, L. Zhang, Z. Si, C. Zhang, Z. Cheng, X. Zhu, *Polym. Chem.* **2013**, *4*, 5664.
- [33] M. Teodorescu, S. G. Gaynor, K. Matyjaszewski, *Macromolecules* **2000**, *33*, 2335.